

Beyond *In Situ* ETEM Imaging: Unveiling the Size-dependent Oxidation Mechanism of Metallic Nanoparticles by Individual Nanoparticle-level Oxidation Kinetic Analysis

Rajat Sainju,¹ Dinithi Rathnayake,² Haiyan Tan,⁴ George Bollas,³ Avinash M. Dongare,¹ Steven L. Suib^{2,4} Yuanyuan Zhu^{1,4*}

¹Department of Materials Science and Engineering, University of Connecticut, Storrs, CT, USA

²Department of Chemistry, University of Connecticut, Storrs, CT, USA

³Department of Chemical & Biomolecular Engineering, University of Connecticut, Storrs, CT, USA

⁴Institute of Materials Science, University of Connecticut, Storrs, CT, USA

* Corresponding author: yuanyuan.2.zhu@uconn.edu

Oxidation of metallic nanoparticles is a fundamental gas-solid reaction, with significant scientific and technological impact in a broad range of applications including catalysis, energy storage, and nanomaterial fabrication. Although establishing reaction models based on kinetic measurements is commonly applied to study the oxidation mechanisms of bulk metals, its feasibility to nanoscale metal particles remains to be validated especially for nanoparticles with different sizes. As a result, a consensus has not yet been reached on the oxidation mechanism of Ni nanoparticle oxidation.

In this work, we utilized *in situ* gas-cell ETEM to directly monitor and quantitatively describe the dynamic oxidation process and kinetics of Ni nanoparticles ranging from 4 to 50 nm under technically relevant 1 bar 1% O₂/N₂ at 600 °C. Our observations revealed distinct structural evolution during the oxidation and different morphology of the product NiO, both depending strongly on the size of the starting Ni nanoparticles. To gain a mechanistic understanding of the Ni nanoparticle oxidation and its size dependence, we performed nanoparticle size distribution quantification, oxidation kinetic measurements, and complementary microstructural analysis. **Figure 1** presents an overview of the 207 Ni nanoparticles whose oxidation kinetics was characterized in both a collective manner by *in situ* selected area electron diffraction (SAED) and selectively at an individual nanoparticle-level by *in situ* ETEM imaging. Specifically, the SAED-based kinetic curve α_{NiO} (black line) is a collective property that averages over all the 207 Ni nanoparticles included by the SAED aperture, presenting an overall oxidation duration of ~ 80 s. In contrast, the oxidation data extracted from selected individual nanoparticles (marked by squares) exhibit a wide range of oxidation durations from 1 s to over 1 min (**Table 1**), suggesting reaction heterogeneity. To extract nanoparticle-level kinetic curves, selected large Ni nanoparticles were tracked in *in situ* images and carefully segmented for the three phases presented – metal (green), oxide (red), and voids (turquoise). Then, the NiO area curve $A_{\text{NiO}}(t)$, normalized NiO volume fraction curve $\alpha_{\text{NiO}}(t)$ and effective NiO thickness curve $X_{\text{NiO}}(t)$ were calculated based on the segmented areas using a home-written MATLAB script. By quantifying NiO thickness/volume change in real space, individual nanoparticle-level oxidation kinetics was established and directly correlated with nanoparticle microstructural evolution with specified fast oxidation directions.

Interestingly, The NiO area curve $A_{\text{NiO}}(t)$ (Figure 1 right) suggests two different oxidation stages characterized by an obvious drop in oxidation rate. Through kinetic model fitting and complementary microstructural evolution examination at an individual nanoparticle level, we propose a unified oxidation theory with a two-stage oxidation process — stage 1: dominated by the early NiO nucleation (Avrami-Erofeev model) and stage 2: the Wagner diffusion-balanced NiO shell thickening (Wanger

model). For the Ni nanoparticles whose radii are smaller than the critical thickness under our oxidation condition, their oxidation ceases at stage 1 without proceeding into the formation of Kirkendall voids and thus produces homogeneous spherical NiO. For larger Ni nanoparticles, i.e., starting radii are larger than the critical thickness, their oxidation proceeds into stage 2 and leads to the formation of hollow NiO shells. In turn, a comparison between the collective and the nanoparticle-level kinetic curve fitting found that the former is probably skewed by the contributions of the small and medium Ni nanoparticles that oxidized early (marked by green and turquoise arrows in Figure 1), and thus influences the curve fitting outcome. This suggests that for nanoparticles with different sizes it may not be sensible to directly associate the collective kinetic data with one oxidation model of averaged nanoparticle size [1].

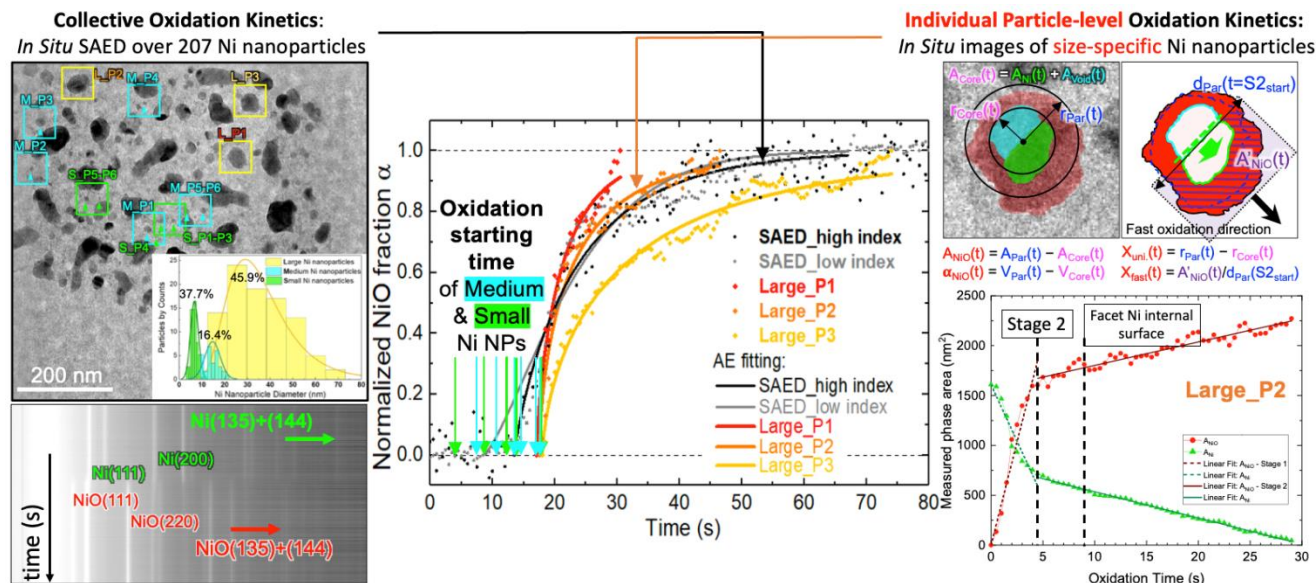


Figure 1. Comparison between the collective SAED-based oxidation kinetic curve and the individual nanoparticle-level image-based oxidation kinetic curve.

Ni NP Oxidation by type	Stage 1								Stage 2								Time END (s)	Full Oxidation Duration (s)
	Time Start1 (s)	Duration_Stage1 (s)	Ni NP diameter_S tart1 (nm)		NiO (shell) thickness /NiO diameter _END1 (nm)		Time_Start2 (s)	Duration_Stage2 (s)	Ni Core diameter_ Start2 (nm)		NiO (shell) thickness_E ND2 (nm)							
Type 1: Large	L_P1	17	2.5	3.5	42.9	43.8	5.9	8.5	19.5	12.5	31.5	31.3	30.7 ± 0.5	23.4	24.6	32	15	35.0
	L_P2	17.5	4.5	± 1.0	45.3	± 1.3	11.9	± 3.0	22	26	± 31.5	30.2	± 0.5	23.9	± 1.8	48	30.5	± 22.6
	L_P3	18	3.5	± 1.0	43.2	± 1.3	7.8	3.0	21.5	56	22.3	30.6	± 0.5	26.7	± 1.8	77.5	59.5	± 22.6
Type 2: Medium	M_P1	18	1.5	± 1.1	16.5	± 4.8	N/A	N/A	19.5	0.5	6.6	N/A	N/A	6.4	± 1.6	20	2	± 9.3
	M_P2	17	1.5	± 1.1	10.6	± 4.8	N/A	N/A	18.5	5.5	± 6.6	N/A	N/A	3.9	± 1.6	24	7	± 9.3
	M_P3	14.5	4.5	± 1.1	22.6	± 4.8	N/A	N/A	19	6.5	± 4.1	N/A	N/A	7.8	± 1.6	25.5	11	± 4.6
	M_P4	11	3	± 1.1	9.2	± 4.8	N/A	N/A	14	5.5	± 4.1	N/A	N/A	3.6	± 1.6	19.5	8.5	± 4.6
	M_P5	8.5	2.5	± 1.1	13.6	± 4.8	N/A	N/A	11	13	± 4.1	N/A	N/A	5.1	± 1.6	24	15.5	± 4.6
	M_P6	14	3	± 1.1	13.5	± 4.8	N/A	N/A	17	8.5	± 4.1	N/A	N/A	4.4	± 1.6	25.5	11.5	± 4.6
Type 3: Small	S_P1	12.5	1	± 0.5	11.2	± 3.0	13.4	10.8	N/A	N/A	N/A	N/A	N/A	N/A	N/A	13.5	1	± 0.5
	S_P2	14.0	1	± 0.5	10.6	± 3.0	12.5	± 4.3	N/A	N/A	N/A	N/A	N/A	N/A	N/A	15	1	± 0.5
	S_P3	12.5	0.5	± 0.5	6.9	± 3.0	8.5	± 4.3	N/A	N/A	N/A	N/A	N/A	N/A	N/A	13	0.5	± 0.5
	S_P4	9.0	1	± 0.5	5.7	± 3.0	6.9	± 4.3	N/A	N/A	N/A	N/A	N/A	N/A	N/A	10	1	± 0.5
	S_P5	4.5	2	± 0.5	5.1	± 3.0	6.2	± 4.3	N/A	N/A	N/A	N/A	N/A	N/A	N/A	6.5	2	± 0.5
	S_P6	18	1	± 0.5	12.0	± 3.0	17.1	± 4.3	N/A	N/A	N/A	N/A	N/A	N/A	N/A	19	1	± 0.5

Table 1. Oxidation duration and NiO thickness for the Stage 1 and Stage 2 oxidation of representative Ni nanoparticles (marked by squares in Figure 1) categorized by the initial Ni nanoparticle size.

References:

[1] The authors acknowledge the ACS Petroleum Research Fund (Grant No. PRF# 61719-DNI10).